Accuracy and convergence properties of multiple-scattering theory in three dimensions

W. H. Butler
Metals and Ceramics Division, Oak Ridge National Laboratory, P.O. Box 2008, Oak Ridge, Tennessee 37831-6114

X.-G. Zhang
Department of Chemistry and Materials Sciences, Lawrence Livermore National Laboratory, Livermore, California 94550

(Received 14 January 1991)

We present a numerical and analytical study of the accuracy and convergence properties of multiple-scattering theory (MST) in three dimensions. The convergence with respect to the number of angular momentum states, $\ell_{\max}$, of the solutions to the three-dimensional MST equations for two muffin-tin potentials is studied analytically and by means of numerical calculations. The rate of convergence appears to be a universal quantity which depends, in the limit of $\ell_{\max} \to \infty$, only on the separation between the scatterers relative to their radii. No evidence of error in the energy, the wave function, or the derivative of the wave function in the limit $\ell_{\max} \to \infty$ is found. In numerical tests which use square-well potentials and truncated Coulomb potentials it is found that the accuracy of the calculated wave functions and their derivatives is limited by the precision with which real numbers can be represented on the digital computers available to the authors (approximately one part in 10^{28}) rather than by postulated errors inherent in MST. Analytic formulas, valid in the limit of large $\ell_{\max}$, for the residual errors in the solutions of the MST equations indicate that these errors vanish in the limit $\ell_{\max} \to \infty$. These results are inconsistent with the claim of Badralexe and Freeman [Phys. Rev. B **37**, 10469 (1988); **41**, 10226 (1990)] that multiple-scattering theory does not yield exact solutions to the wave equation for muffin-tin potentials.

I. INTRODUCTION

Although multiple-scattering theory (MST) has been used for nearly a century to solve some of the fundamental partial differential equations of mathematical physics,[1–5] we know of no careful study of its accuracy and convergence properties in the limit in which a large number of angular momentum states are used to represent the solutions to the differential equation. This paper contains such a study for the case of two muffin-tin scatterers in three dimensions.

There are several reasons why such a study might be useful. One reason concerns ongoing research aimed at eliminating the restriction of MST to muffin-tin potentials. It is becoming increasingly clear, at least to the present authors,[6,7] that there is no difficulty in principle with the extension of MST to general, space filling potentials, but there are difficulties in practice which relate to the the conditional and slowly convergent angular momentum sums which may arise in such an extension. A careful study of the muffin-tin case provides a useful foundation and a baseline against which the convergence and accuracy of the general case may be compared.

A second reason relates to the controversy that has arisen concerning work by Badralexe and Freeman who claim that MST is incorrect even for muffin-tin scatterers.[8] Although the Badralexe-Freeman paper has been strongly challenged,[9] its authors continue to defend their position.[10] In an attempt to shed some light on this controversy one of us earlier investigated the validity and accuracy of multiple-scattering theory by using it to solve the wave equation for one- and two-dimensional model systems.[11] In that study it was demonstrated that MST is exact in one dimension and that any errors in two dimensions must be extremely small (less than one part in 10^{15} for the wave function).

In the present paper we present what we believe is a careful analysis of the bound states of three-dimensional systems using multiple-scattering theory. The particular model system which we use to test MST consists of two muffin-tin potentials in free space. This particular choice seemed appropriate to us because of its simplicity and because it was in the context of this system that Badralexe and Freeman derived their "proof" that MST is incorrect.

By its very nature the MST representation for the wave function is very amenable to numerical checks of its accuracy and validity. This is because, as we show below, the MST secular equation may be viewed as a self-consistency condition which fits together two or more local solutions to a partial differential equation in such a way that the global solution satisfies the boundary conditions and is smooth and continuous everywhere. If these easily verifiable conditions are satisfied then the solution is undoubtedly correct.

By careful attention to the numerical aspects of our

calculations (including the use of quadruple precision, i.e., 128 bit, computer arithmetic) we are able to obtain by direct calculation, upper bounds to possible errors inherent in MST for the model systems which we have considered. We find that these upper bounds are zero within the numerical precision (approximately 28 decimal digits) available to us. We also report analytic expressions for the *rate* of convergence of the angular momentum expansions associated with multiple scattering theory for these systems. These expressions indicate that the error in an MST calculation can be reduced to zero by use of a sufficiently large number of angular momentum states. These expressions, and our numerical results also indicate that the rate of convergence of the angular momentum expansions varies greatly with the ratio of the distance between the scatterers to the muffin-tin radius, a fact which may have an impact on strategies for efficiently implementing full-potential MST.

Section II contains a brief recapitulation of the formalism necessary to treat two muffin-tin scatterers using multiple-scattering theory. Section III presents the results of our numerical studies of the accuracy and convergence of multiple-scattering theory when applied to two test systems consisting of two square well potentials and two truncated Coulomb potentials, respectively. Results for the convergence of the energy, the wave function, and the derivative of the wave function are reported.

Section IV contains an analysis of how the errors in an MST calculation decrease as the number of angular momentum states increases. There we report analytic expressions, valid in the limit of a large number of angular momentum states, for the rate of decrease of the errors in MST. The convergence rate in this limit appears to be a universal quantity depending only on the separation of the scatterers and their radii. Section V contains a summary of our conclusions and a discussion of their implications.

II. THE TWO-SCATTERER PROBLEM IN THREE DIMENSIONS

Our objective is to solve the time-independent Schrödinger equation, which (in atomic units) is given by

$$[-\nabla^2 + V(\mathbf{r}) - E]\Psi(\mathbf{r}, E) = 0 \ , \tag{1}$$

for the special case where the potential $V(\mathbf{r})$ has the "muffin-tin" form; that is, it consists of a sum of nonoverlapping, spherically symmetrical potentials,

$$V(\mathbf{r}) = \sum_n v_n(\mathbf{r} - \mathbf{R}_n) \ . \tag{2}$$

Since we will only be concerned with two potentials in this paper it will be convenient to denote them by A and B. It is helpful to think of space as being divided into two regions in such a way that region I consists of those points "inside" one of the potentials, i.e., those points where $V(\mathbf{r})$ is nonzero, and region II consists of those points "outside" all of the potentials, i.e., those points where $V(\mathbf{r})$ vanishes. Region I, for the particular case of two scatterers, is composed of two pieces, IA inside potential A and IB inside potential B (Fig. 1).

The basic idea of MST is to solve the wave equation separately in the region inside each scatterer (regions IA and IB) and in the region outside all scatterers (region II) and then to fit these partial solutions together into a solution that is acceptable over all of space by matching the pieces at the boundaries of each region. Thus we write solutions for regions IA and IB as

$$\Psi_{\mathrm{I}n} = \sum_L c_L^n R_\ell^n(r_n) Y_L(\hat{\mathbf{r}}_n) \ , \quad n = (A, B) \tag{3}$$

and for region II as

$$\Psi_{\mathrm{II}} = \sum_{n=A,B} \sum_L b_L^n \tilde{h}_\ell(z_n) Y_L(\hat{\mathbf{r}}_n) \ . \tag{4}$$

In the above two equations and below, L (which labels the spherical harmonic Y_L) denotes the combination of orbital and azimuthal quantum numbers $\{\ell, m\}$ and a sum over L is to be interpreted as $\sum_{\ell=0}^{\infty} \sum_{m=-\ell}^{\ell}$. The notations r_n and $\hat{\mathbf{r}}_n$ indicate, respectively, distances and directions measured from the center of site n, while the notation z_n is used as a shorthand for κr_n where $\kappa = \sqrt{-E}$.

The "inside" functions R_ℓ^n used in region I are solutions of the "radial" part of the wave equation for a single scatterer,

$$[-r_n^{-1}(d^2/dr_n^2)r_n + \ell(\ell+1)/r_n^2 + v_n(r_n) - E]R_\ell^n(E, r_n) = 0 \ , \tag{5}$$

and behave near the origin as r_n^ℓ. The "outside" functions, $\tilde{h}_\ell$, used in region II are solutions of the free space radial equation [Eq. (5) with $v_n = 0$]. Since we are

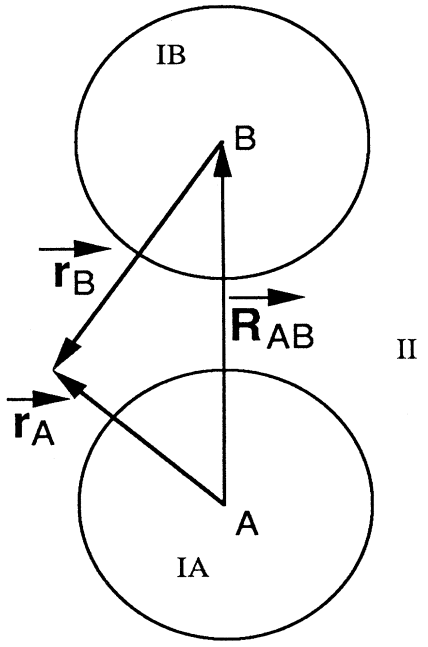

FIG. 1. Two spherical scatterers in three dimensions.

looking for bound states of the two-scatterer problem we must look for states at negative energy relative to the energy zero of region II. Consequently, the functions $\tilde{h}_\ell(z)$ are obtained by analytic continuation of the spherical Hankel functions to imaginary argument. We choose $\tilde{h}_\ell(z) = -i^\ell h_\ell(iz)$. These functions behave as $r_n \to \infty$ as $\tilde{h}_\ell(z_n) \to e^{-z_n}/z_n$. Near the origin these functions behave as $(2\ell-1)!!/z_n^{\ell+1}$.

The MST equations result from the requirement that the wave functions Ψ_{IA} and Ψ_{IB} match smoothly and continuously onto Ψ_{II} at the boundary between regions I and II. In order to satisfy this matching condition it is convenient to define auxiliary functions in region II, Ψ_{IIA} and Ψ_{IIB}, that are single center expansions about the centers of potentials A and B, respectively,

$$\Psi_{IIn} = \sum_L a_\ell^n \tilde{j}_\ell(z_n) Y_L(\hat{\mathbf{r}}_n) + \sum_L b_L^n \tilde{h}_\ell(z_n) Y_L(\hat{\mathbf{r}}_n) \ ,$$

$$n = (A, B) \ . \quad (6)$$

Here $\tilde{j}_\ell$ is obtained from the analytic continuation of the spherical bessel function to imaginary argument, $\tilde{j}_\ell(z) = i^{-\ell} j_\ell(iz)$. The function $\tilde{j}_\ell(z_n)$ behaves near the origin as $z_n^\ell/(2\ell+1)!!$ but is irregular as $r_n \to \infty$, behaving as $e^{z_n}/2z_n$.

It is a relatively simple matter to match Ψ_{IA} to Ψ_{IIA} and to match Ψ_{IB} to Ψ_{IIB}. The coefficient c_L^n can be used to match the magnitude of each partial wave at the muffin-tin radius, r_n^0, and the ratio of a_L^n to b_L^n can be chosen to ensure that the logarithmic derivatives match. This latter condition determines the t matrix, $t_\ell(E)$, although for our purposes it is more convenient to work with the inverse of the t matrix which we denote by $m_\ell(E)$.[12] Thus if m_L^n is defined by

$$a_L^n = m_L^n b_L^n \ , \quad (7)$$

it will be given by

$$m_L^n(E) = m_\ell^n(E) = -\frac{z_n^0 \tilde{h}_\ell'(z_n^0) - r_n^0 \gamma_\ell^n \tilde{h}_\ell(z_n^0)}{z_n^0 \tilde{j}_\ell'(z_n^0) - r_n^0 \gamma_\ell^n \tilde{j}_\ell(z_n^0)} \ , \quad (8)$$

where γ_ℓ^n is the logarithmic derivative of the radial wave function evaluated at the muffin-tin radius, r_n^0,

$$\gamma_\ell^n(E) = \left(\frac{dR_\ell^n(E, r_n)/dr_n}{R_\ell^n(E, r_n)} \right)_{r_n = r_n^0} \quad (9)$$

and where $z_n^0 = \kappa r_n^0$.

It is clear that neither Ψ_{IIA} nor Ψ_{IIB} is an acceptable solution for all of region II since they both contain terms that grow exponentially as $r_n \to \infty$. For the purposes of MST, however, it is only necessary that they be able to accurately represent Ψ_{II} in the vicinity of their respective scatterers. This condition will be satisfied if the following relation holds in the vicinity of scatterer A:

$$\sum_L m_\ell^A b_L^A \tilde{j}_\ell(z_A) Y_L(\hat{\mathbf{r}}_A) = \sum_L b_L^B \tilde{h}_\ell(z_B) Y_L(\hat{\mathbf{r}}_B) \quad (10)$$

and if an analogous relation holds in the vicinity of scatterer B:

$$\sum_L m_\ell^B b_L^B \tilde{j}_\ell(z_B) Y_L(\hat{\mathbf{r}}_B) = \sum_L b_L^A \tilde{h}_\ell(z_A) Y_L(\hat{\mathbf{r}}_A) \ . \quad (11)$$

The final step in deriving the MST equations requires the existence of convergent expansions of the form

$$\tilde{h}_{\ell'}(z_B) Y_{L'}(\hat{\mathbf{r}}_B) = \sum_L \tilde{j}_\ell(z_A) Y_L(\hat{\mathbf{r}}_A) g_{L,L'}(E, \mathbf{R}_{AB}) \quad (12)$$

and

$$\tilde{h}_{\ell'}(z_A) Y_{L'}(\hat{\mathbf{r}}_A) = \sum_L \tilde{j}_\ell(z_B) Y_L(\hat{\mathbf{r}}_B) g_{L,L'}(E, \mathbf{R}_{BA}) \ , \quad (13)$$

where $\mathbf{R}_{AB} = \mathbf{R}_B - \mathbf{R}_A$. It can be shown that such expansions exist if $r_A < R_{AB}$ in Eq. (12) and $r_B < R_{BA}$ in Eq. (13). The expansion coefficients, $g_{L,L'}(E, \mathbf{R})$ are given by

$$g_{L,L'}(E, \mathbf{R}) = 4\pi(-1)^\ell \sum_{L''} C(L, L', L'') \tilde{h}_{\ell''}(\kappa R) Y_{L''}(\hat{\mathbf{R}}) \ , \quad (14)$$

where the Gaunt numbers, $C(L, L', L'')$, are defined in terms of real spherical harmonics by

$$C(L, L', L'') = \int d\hat{\mathbf{r}}\, Y_L(\hat{\mathbf{r}}) Y_{L'}(\hat{\mathbf{r}}) Y_{L''}(\hat{\mathbf{r}}) \ . \quad (15)$$

If $\mathbf{R}_{AB}$ is chosen along the z axis, the z component of the angular momentum is a good quantum number allowing the expansion coefficients to be simplified somewhat,

$$\begin{aligned} g_{L,L'}(E, R\hat{\mathbf{z}}) &= g_{\ell,\ell'}^m(E, R)\delta_{m,m'} \\ &= \sum_{\ell''=|\ell-\ell'|}^{\ell+\ell'} (2\ell''+1) d^m(\ell, \ell', \ell'') \\ &\quad \times \tilde{h}_{\ell''}(\kappa R)(\pm 1)^{\ell''} \\ &\quad \times (-1)^\ell \sqrt{(2\ell+1)(2\ell'+1)} \ , \end{aligned} \quad (16)$$

where the + (−) sign is taken if $\mathbf{R}$ lies along the + (−) z axis and where the "reduced" Gaunt numbers, $d^m(\ell, \ell', \ell'')$ vanish unless $\ell + \ell' + \ell''$ is an even integer; in which case they are given for $m = 0$ (σ) and $m = 1$ (π) states by

$$d^\sigma(\ell, \ell', \ell'') = \int_0^1 dx\ P_\ell(x) P_{\ell'}(x) P_{\ell''}(x) \quad (17)$$

and

$$d^\pi(l, l', l'') = \frac{\int_0^1 dx\ (1-x^2)\ P_\ell'(x)\ P_{\ell'}'(x)\ P_{\ell''}(x)}{\sqrt{\ell\ell'(\ell+1)(\ell'+1)}} \ . \quad (18)$$

Substitution of these equations into Eqs. (10) and (11) yields a set of homogeneous linear equations,

$$m_\ell^A(E)b_\ell^A = \sum_{\ell'} g_{\ell,\ell'}^m(E,\mathbf{R}_{AB})b_{\ell'}^B \ , \tag{19}$$

$$m_\ell^B(E)b_\ell^B = \sum_{\ell'} g_{\ell,\ell'}^m(E,\mathbf{R}_{BA})b_{\ell'}^A \ . \tag{20}$$

These are the MST equations.

The energies for which these equations have a solution are the eigenvalues of Eq. (1) and the solution vector b_L^n determines the wave function through Eq. (4) in region II and through Eqs. (3) and (6) in region I. If the scatterers are identical, $m^A = m^B$, further simplification is possible, since, in that case, the wave functions for the A and B scatterers are related by symmetry, being either symmetric or antisymmetric with respect to inversion through the midpoint of the line joining their centers. States that are symmetric with respect to inversion are denoted as *gerade* by the spectroscopists and states that are antisymmetric with respect to inversion are labeled *ungerade*. Thus the coefficients of the expansions about the A and B sites are related by

$$b_\ell^B = (\pm 1)\ (-1)^\ell b_\ell^A \ , \tag{21}$$

where the (+) sign is appropriate for the symmetric (g) states and the (−) sign is appropriate for the antisymmetric (u) states. This simplification allows the MST equations for a homonuclear diatomic system to be written as

$$\sum_{\ell'}[m_\ell^A(E)\delta_{\ell,\ell'} - g_{\ell,\ell'}^m(E,S)(\pm 1)(-1)^{\ell'}]b_{\ell'}^A = 0 \ . \tag{22}$$

Here we have used S to represent $|\mathbf{R}_{AB}|$, the separation between the scatterers. In practice, when these equations are solved numerically, it is necessary to truncate the infinite system of linear equations. When this is done the energy and the wave-function coefficients will depend on $\ell_{\max}$ the maximum value of ℓ used in the solution of the symmetric, homogeneous, linear system,

$$\sum_{\ell'=0}^{\ell_{\max}}[m_\ell^A(E_{\ell_{\max}})\delta_{\ell,\ell'} - g_{\ell,\ell'}^m(E_{\ell_{\max}},S)(\pm 1)(-1)^{\ell'}]$$

$$\times b_{\ell'}^A(\ell_{\max}) = 0 \quad (\ell = 0,1,\ldots,\ell_{\max}) \ . \tag{23}$$

III. RESULTS OF NUMERICAL STUDIES OF CONVERGENCE AND ACCURACY OF MST

We have solved the two-scatterer MST equations both for spherical square-well potentials and for truncated Coulomb potentials. For a square-well potential of depth V, Eq. (9) becomes

$$\sqrt{E+V}\,j_\ell'(\sqrt{E+V}r^0)/j_\ell(\sqrt{E+V}r^0) \ , \tag{24}$$

where r^0 is the radius of the square well. For the problem of two identical spherical square wells we can take r^0 to be unity without loss of generality if the separation S is measured in units of r^0 and if E and V are measured in units of $1/(r^0)^2$. Table I gives some of the calculated bound-state energies obtained by solving the MST equations. In most cases these energies were calculated with a precision that exceeded 27 decimal digits, although only 16 significant figures are included in the table. For reasons which we will discuss below, we believe that the calculated energies are *accurate* to 27 digits as well.

The $1\sigma_g$ and $1\sigma_u$ states of Table I were calculated for a potential of depth $V = 5$. An isolated potential of this depth has only one bound state. The $2\sigma_g$ states and $1\pi_u$ states were calculated with a potential of depth $V = 10$. These states of the diatomic molecule are derived from the second bound state of this potential. A third state for the diatomic molecule, the $2\sigma_u$ state, is derived from the second bound state of the isolated potential, but this state increases in energy and becomes unbound (for our choices of r^0 and V) as the potentials are brought together.

Figure 2 shows how the energy converges as a function of the number of angular momentum states for various values of the separation for the $1\sigma_g$, $1\sigma_u$, $2\sigma_g$, and $1\pi_u$ states. Figure 3 shows how the wave function and its normal derivative converge for these same states.

In the case of the energy, the numbers plotted are the differences between $E(\ell_{\max})$ and $E(\infty)$ which in practice is obtained by increasing $\ell_{\max}$ until $E(\ell_{\max})$ is constant within the precision of the computer. For the wave function and its derivative, however, the plotted numbers are the relative root mean square differences between Ψ_{IA}, Eq. (3), and Ψ_{II}, Eq. (4), averaged over the surface of scatterer A. The relative root mean square error of the wave function referred to in Fig. 3, for example, is

$$\left(\frac{\int dS_A(\Psi_{IA}-\Psi_{II})^2}{\int \Psi_{II}^2 dS_A}\right)^{1/2} \ . \tag{25}$$

The corresponding quantity with the wave functions replaced by their normal derivatives with respect to r is also plotted in Fig. 3.

If these differences in the wave function and its normal derivative vanish at the boundary between regions I and II we have obtained the correct solution to the Schrödinger equation. Recall that the Ψ_{In} is a superposition of terms each of which satisfies the Schrödinger equation by construction in region In and is regular in that region. Similarly, each term of Ψ_{II} satisfies the Schrödinger equation in all of region II, is regular in that region, and satisfies the boundary condition at $r \to \infty$. Since the Schrödinger equation is a linear partial differential equation, a sum of solutions is also a solution. If the wave function and its derivative are continuous everywhere then it must be an acceptable solution to the Schrödinger equation.[13] The only points at which the continuity and smoothness of the wave function could be

TABLE I. Energies calculated for two spherical square-well potentials. The depth of the potential, V, is $5/(r^0)^2$ for the $1\sigma_g$ and $1\sigma_u$ states and is $10/(r^0)^2$ for the $2\sigma_g$ and $1\pi_u$ states. The energy is measured in in units of $1/(r^0)^2$.

S	$1\sigma_g$	$1\sigma_u$	$2\sigma_g$	$1\pi_u$
2.0	−1.326 675 638 612 688	−0.507 986 435 475 966 5	−0.704 813 227 629 546 8	−0.336 669 578 151 853 3
2.4	−1.144 684 789 098 379	−0.683 556 737 750 893 5	−0.389 781 254 990 707 5	−0.201 010 637 832 359 3
3.0	−1.026 932 973 585 779	−0.821 949 198 199 346 2	−0.213 083 529 443 594 7	−0.122 088 180 300 462 5
4.5	−0.946 974 739 131 619 4	−0.915 127 306 308 885 1	−0.095 170 907 449 155 17	−0.068 543 603 913 377 09
6.0	−0.932 413 720 472 693 4	−0.928 602 714 280 335 0	−0.067 765 484 341 664 43	−0.056 489 155 188 061 57
∞	−0.931 426 119 417 670 1	−0.931 426 119 417 670 1	−0.049 665 725 017 485 42	−0.049 665 725 017 485 42

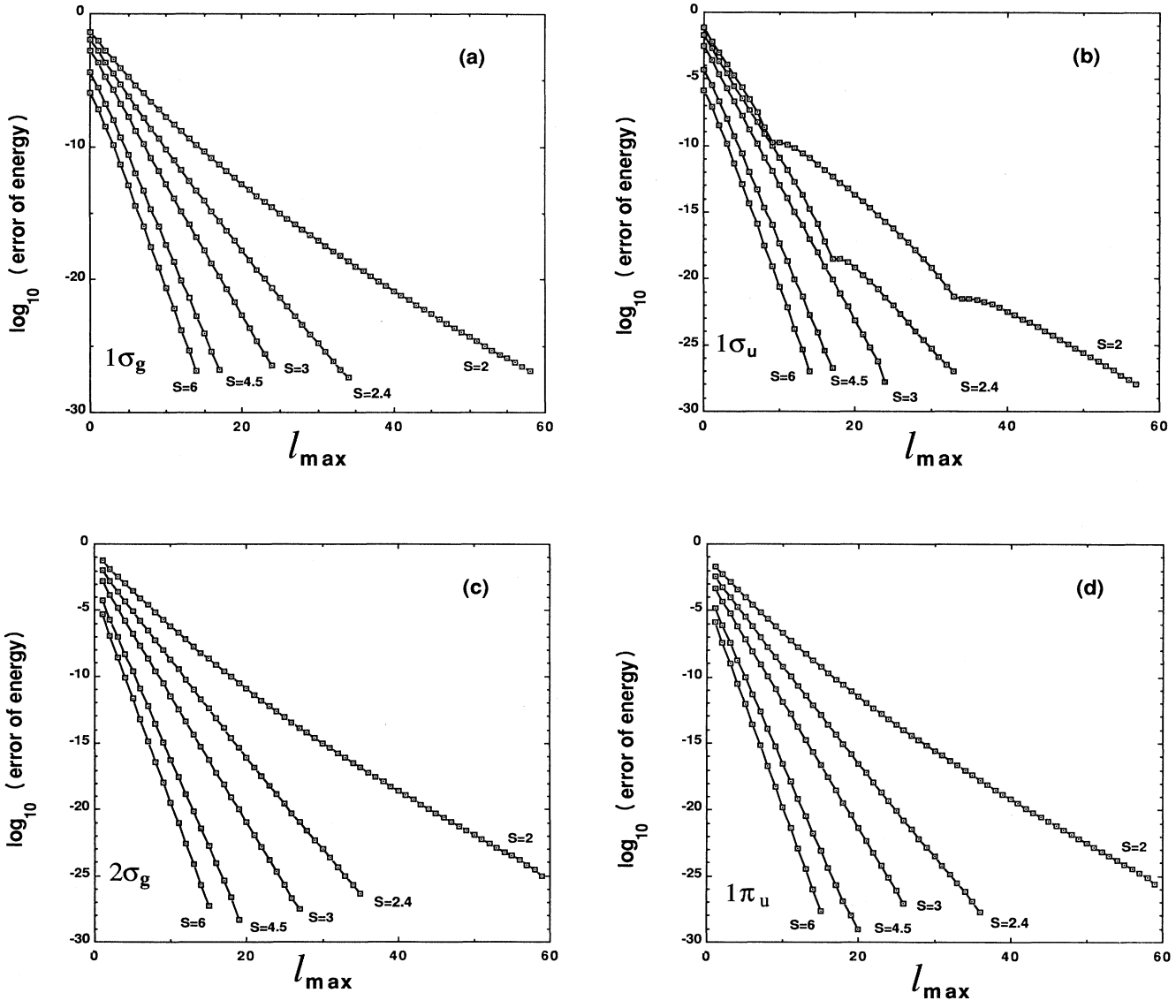

FIG. 2. Convergence of the bound-state energy for a molecule consisting of two spherical square-well potentials. S labels the separation between the centers of the potentials in units of the muffin-tin radius r^0 so that $S = 2$ indicates touching spheres. The ordinate is the logarithm (base 10) of the difference between $E_{\ell_{\max}}$ and the converged bound-state energy. (a) $1\sigma_g$ state for $V = 5$. (b) $1\sigma_u$ state for $V = 5$. (c) $2\sigma_g$ state for $V = 10$. (d) $1\pi_u$ state for $V = 10$.

questioned are those at the surfaces that separate regions I and II.

From Figs. 2 and 3 it can be seen that the energy, the wave function, and the normal derivative of the wave function all converge in an approximately exponential manner. The error decreases by a factor that varies only slightly every time $\ell_{\max}$ is increased. There are, however, two exceptions to this rule. First, the slopes of the curves in Figs. 2 and 3 sometimes vary significantly for small values of $\ell_{\max}$ giving some curvature to the semilogarithmic plots. The detailed behavior of the curves for small values of $\ell_{\max}$ may depend on the potential and on the nature of the particular state. The second exception is the strange behavior of the convergence curves for the $1\sigma_u$ state which is caused by the wave-function coefficients b_ℓ^A changing sign at certain values of ℓ.

It is not surprising that the coefficients b_ℓ^A change sign at certain values of ℓ for states such as the $1\sigma_u$ which are antisymmetrical with respect to inversion in the plane which perpendicularly bisects the line joining the centers of the potentials. In order to understand qualitatively how these sign changes can occur, it is interesting to compare the wave functions for the $1\sigma_g$ and $1\sigma_u$ states along the line connecting their centers. It is well known[14] that relative to overlapped atomic orbitals, the symmetric states such as the $1\sigma_g$ concentrate additional

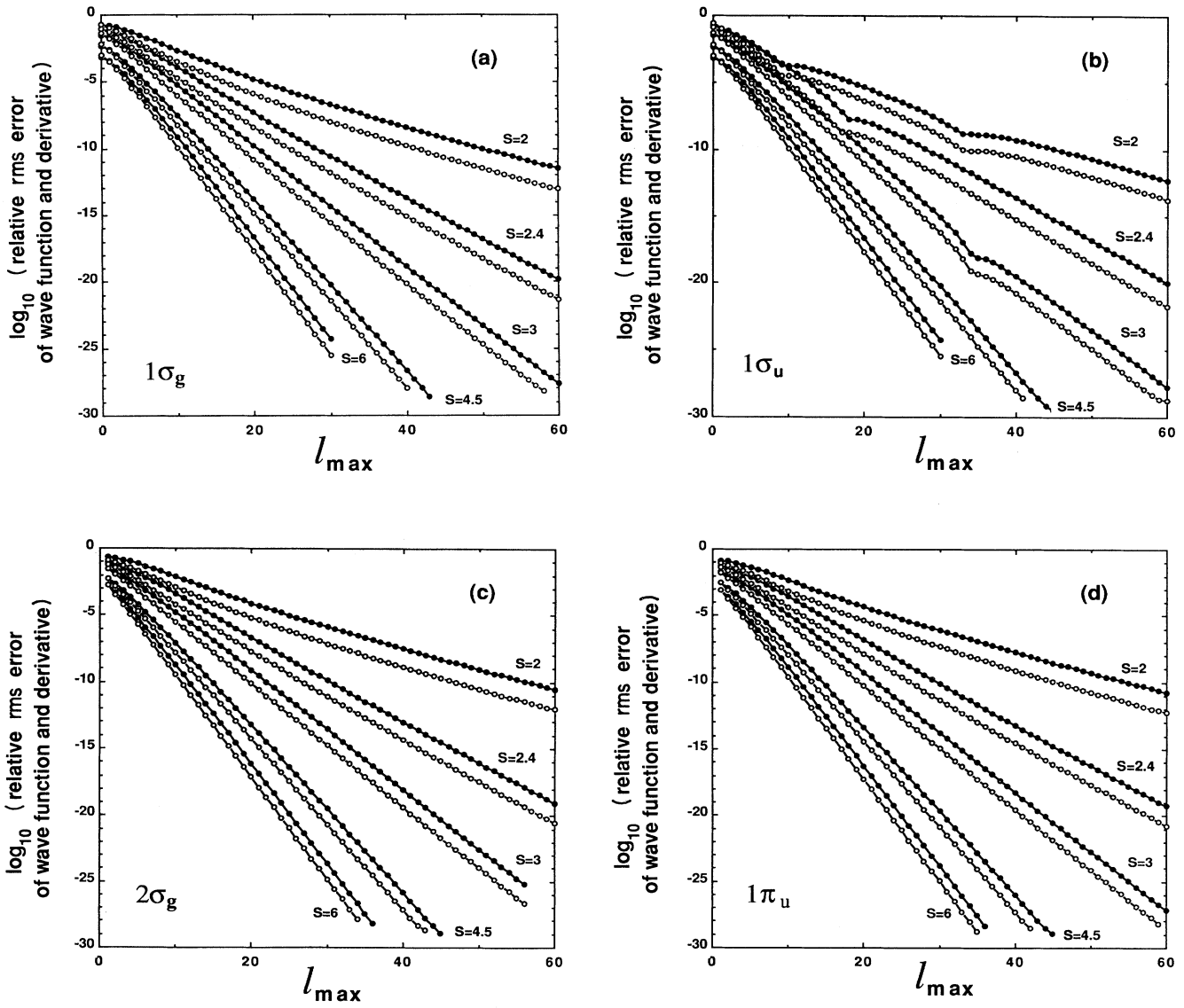

FIG. 3. Logarithm (base 10) of the relative root-mean-square error of the wave function (open circles) and of the normal derivative of the wave function (filled circles) for a molecule consisting of two square-well potentials. The square of the relative error in the wave function or normal derivative at the muffin-tin radius has been averaged over the surface of one of the scatterers. It is the logarithm of the square root of this quantity which is plotted. (The parameters are the same as for Fig. 2.)

charge density between the atoms while the antisymmetric states such as the $1\sigma_u$ expel charge. An $\ell_{\max} = 0$ calculation corresponds (for the $1\sigma_g$ and $1\sigma_u$ states) to overlapping atomic orbitals, and so we can say that the coefficients of the $\ell > 0$ partial waves must have the proper sign to add additional charge between the atoms for the symmetric states and to expel charge for the antisymmetric states. The physical reason for the difference in the two cases is the additional kinetic energy required by the antisymmetric state which can be reduced by relaxing the wave function outward from the center of the molecule.

The relationship between the increase or decrease in amplitude in the vicinity of the scatterers and the sign of the coefficient b_ℓ^A can be understood in terms of the behavior of the functions $\tilde{h}_\ell(z)$. For all ℓ, $\tilde{h}_\ell \to e^z/z$ as $z \to \infty$, however, their behavior at the origin depends strongly on ℓ with the higher-order functions diverging much more strongly, i.e., $\tilde{h}_\ell(z) \to (2\ell-1)!!/z^{\ell+1}$ as $z \to 0$. This means that if the coefficients b_ℓ^A all have the same sign, each additional partial wave will concentrate more amplitude near the scatterers and decrease the amplitude at large distances. Thus it is clear that the coefficients b_ℓ^A for the $1\sigma_u$ states must change sign. In fact, b_1^A and some higher ℓ coefficients differ in sign from b_0^A for the $1\sigma_u$ state. The additional sign reversals occur at values of ℓ which depend on S and presumably are necessary to ensure a perfect match of the wave functions.

As the value of b_ℓ^A passes through zero one has a situation where an additional partial wave makes no difference to the accuracy of the calculation. This leads to the dips in the convergence curves of the $1\sigma_u$ states for $S = 2r^0$, $2.4r^0$, and $3r^0$ seen in Figs. 2(b) and 3(b). If this effect is ignored, the convergence curves for the $1\sigma_u$ states are almost identical to those for the $1\sigma_g$ states.

It is easily seen by comparing Fig. 2 with Fig. 3 that the energy converges much faster than the wave function or its derivative. This is entirely in conformity with our expectations since the MST equations were derived from a variational principle by Kohn and Rostoker[3] who showed that the error in the energy is second order in the relative error of the wave function. As a rough rule of thumb we find that for the first few values of $\ell_{\max}$, the error in the the wave function and its derivative varies as $(r^0/S)^{\ell_{\max}}$ while the energy converges as the square of this quantity. The *rate* of convergence in the limit of large $\ell_{\max}$ will be discussed in the next section.

Most of the calculations were performed using $\ell_{\max} \leq 60$. This value of $\ell_{\max}$ was sufficient to converge the energies to approximately 28 decimal digits which is the approximate precision with which real numbers can be represented on the computer that we used. For the larger separations, $\ell_{\max} \leq 60$ was sufficient to reduce the relative root mean square errors in the wave functions and their normal derivatives to zero within a tolerance of a few times the computer's precision. For separations of $S = 2r^0$ and $S = 2.4r^0$, however, the discontinuities in the wave function and normal derivative were still computationally significant at $\ell_{\max} = 60$, so we extended the calculations for those separations for the $1\sigma_g$ state to higher values of $\ell_{\max}$. The results are shown in Fig. 4, and

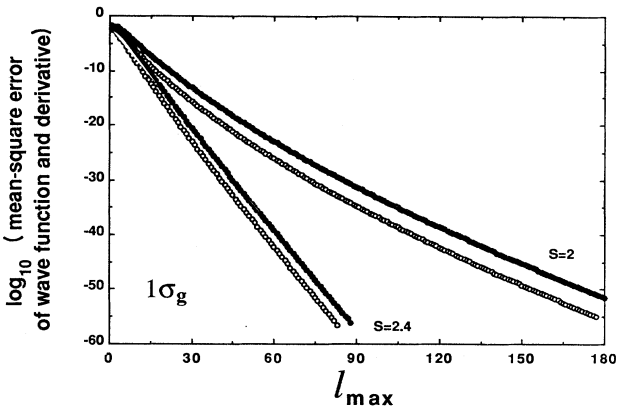

FIG. 4. Logarithm (base 10) of the relative mean-square error of the wave function (open circles) and its normal derivative (filled circles) calculated for $\ell_{\max} \leq 180$ for the $1\sigma_g$ state calculated for $S = 2.4r^0$ and $S = 2r^0$ (touching spheres).

demonstrate that even for touching muffin-tin spheres, there exists a value of $\ell_{\max}$ for which there are no discernible, computationally significant errors in the MST wave function or normal derivative.

It may be useful to emphasize that 10^{-28} is a small number. An accuracy of 1 part in 10^{28} corresponds roughly to measuring the distance from the Earth to the sun with an error that is less than one ten millionth of the diameter of an atom. It should also be clear by comparison of Figs. 2 and 3 as well as from the discussion of the next section, that the error in the energy is approximately equal to the relative mean-square error in the wave function. Thus the error in the energy is of order one part in 10^{56} when the error in the wave function is of order one part in 10^{28}.

We also calculated the bound-state energies and wave functions for a truncated Coulomb potential. Since we were interested in what effect the presence or absence of a discontinuity in the potential at the muffin-tin radius had on the rate of convergence of the MST equations, we eliminated the discontinuity for this test to achieve maximum contrast with the square-well results. The discontinuity was eliminated by shifting the potential so that it vanished at r^0,

$$v(r) = \begin{cases} -2Z(1/r - 1/r^0) & \text{if } r \leq r^0 \\ 0 \text{ otherwise.} \end{cases} \tag{26}$$

There remains, of course, a discontinuity in the slope of the potential at $r = r^0$.

The convergence curves for the energy, wave function, and wave function derivative for the $1\sigma_g$ state of a diatomic molecule with such a Coulomb potential are shown in Fig. 5. The particular parameters used for this calculation were a nuclear charge Z of 2 and a muffin-tin radius of 1 in atomic units. Thus the individual atomic potentials were those of a helium nucleus, chopped off at the Bohr radius of a hydrogen atom and shifted upward by 4 Ry. The bound-state energies are given in Table II.

Although the curves of Fig. 5 are qualitatively very similar to those for the $1\sigma_g$ states of Figs. 2 and 3 there

is a significant improvement in the overall rate of convergence of the energies, the wave functions, and their normal derivatives for the truncated Coulomb potentials in comparison with those for the square-well potentials. This improvement is especially pronounced for the case of touching muffin-tin spheres, $S = 2$. For the larger separations the improvement is less dramatic and it appears that the *rate* of convergence, i.e., the slopes of the curves, are essentially the same for large values of $\ell_{\max}$. The reasons for this behavior will be discussed in the next section.

The convergence curves presented in Figs. 2–5 are qualitatively very similar to those obtained previously in a study of a two-dimensional model system[11] and indicate that MST can be used to obtain an extremely accurate solution to the Schrödinger equation. Although it is seldom necessary to calculate wave functions to higher accuracy than 28 significant digits in condensed matter physics, it is still an interesting exercise to investigate the convergence of MST in the limit of $\ell_{\max} \to \infty$ and to determine whether or not MST is exact in that limit. An analysis of these questions is presented in the following section.

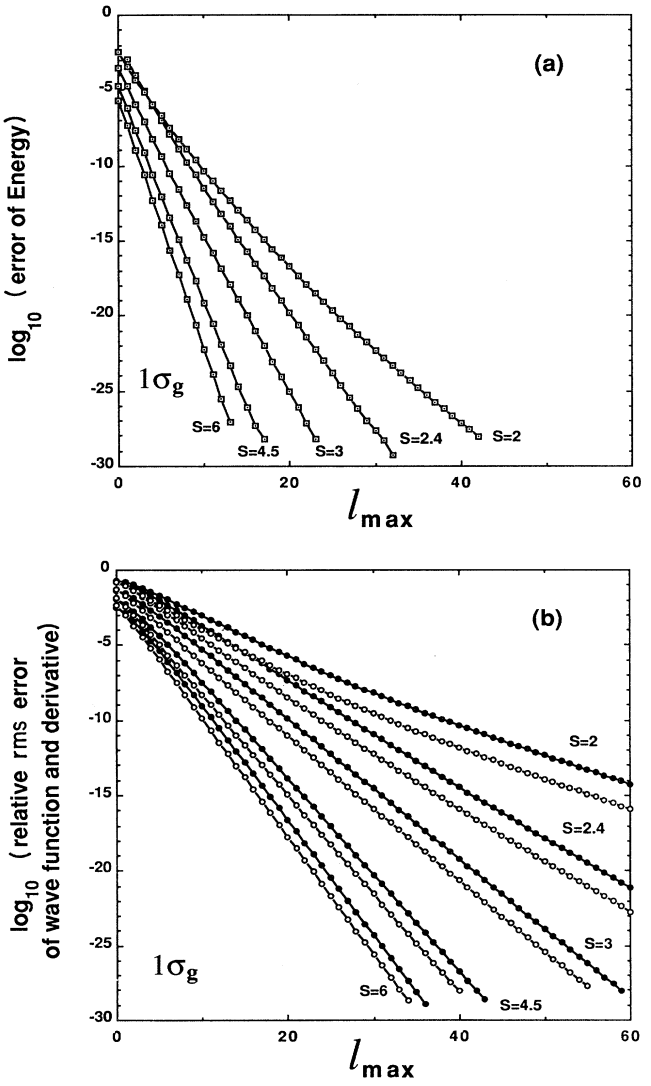

FIG. 5. Convergence of the energy, wave function, and wave-function derivative for the $1\sigma_g$ state calculated using truncated Coulomb potentials of form $(2Ze^2/r) - (2Ze^2/r^0)$ for $r < r^0$, and 0 for $r > r^0$. The nuclear charge Z is taken to be 2 and r^0 is taken to be 1. Panel (a) shows the convergence of the energy and panel (b) shows the convergence of the wave function (open circles) and its normal derivative at the muffin-tin radius (filled circles).

TABLE II. Energies calculated for two truncated Coulomb potentials.

S	$1\sigma_g$
2.0	−0.577 460 001 893 329 8
2.4	−0.497 789 946 700 468 5
3.0	−0.433 057 999 207 138 9
4.5	−0.372 439 806 240 446 9
6.0	−0.355 616 310 673 397 3
∞	−0.347 669 684 989 694 0

IV. ANALYTIC STUDY OF THE CONVERGENCE PROPERTIES OF MST

In this section we present analytic expressions for the dependence of the errors of the MST bound-state energies and wave functions on the angular momentum cutoff, $\ell_{\max}$. Although our analysis is limited to bound states and to the case of two scatterers, we believe that our estimate of the errors in the two-scatterer problem should provide a good indication of the accuracy of MST.

We first consider the accuracy of the bound-state energy calculated with an angular momentum truncation, $\ell_{\max}$. We denote the truncation error of this bound-state energy by $E_{\ell_{\max}} - E_\infty$, where E_∞ is the bound-state energy given by the MST equations in the limit $\ell_{\max} \to \infty$. It is convenient to rewrite Eq. (23) as

$$M^{\ell_{\max}}(E,S)\, B^A(\ell_{\max}) = 0 \ , \tag{27}$$

where $B^A(\ell_{\max})$ is a vector consisting of $b^A_\ell(\ell_{\max})$, and $M^{\ell_{\max}}(E,S)$ is a matrix with elements,

$$M^{\ell_{\max}}_{\ell,\ell'}(E,S) = m^A_\ell(E)\delta_{\ell,\ell'} - g^m_{\ell,\ell'}(E,S)(\pm 1)(-1)^{\ell'}$$

$$(\ell,\ell' = 0,1,\ldots,\ell_{\max}) \ . \tag{28}$$

Obviously, $B^A(\ell_{\max})$ is the eigenvector of $M^{\ell_{\max}}(E,S)$ corresponding to the eigenvalue 0. We now define an $\ell_{\max} \times \ell_{\max}$ matrix, P, which contains all eigenvectors of $M^{\ell_{\max}}(E,S)$. Since $M^{\ell_{\max}}(E,S)$ is symmetric, we have

$$P^{-1} = P^T \tag{29}$$

and

$$\sum_{\ell,\ell'} P_{\ell,i}\, M^{\ell_{\max}}_{\ell,\ell'}(E,S)\, P_{\ell',j} = \alpha_i^{\ell_{\max}}(E)\delta_{i,j} \ , \tag{30}$$

where $\alpha_i^{\ell_{\max}}(E)$ are the eigenvalues of $M^{\ell_{\max}}(E,S)$, and $\alpha_0^{\ell_{\max}}(E_{\ell_{\max}}) = 0$. The error in the energy can be estimated through the expression

$$E_{\ell_{\max}} - E_\infty = \alpha_0^\infty(E_{\ell_{\max}}) \Big/ \left(\frac{d\alpha_0^\infty(E)}{dE}\right)_{E=E_{\ell_{\max}}} . \tag{31}$$

It now remains to find $\alpha_0^\infty(E_{\ell_{\max}})$. We partition the matrix, $M^\infty(E,S)$, into

$$M^\infty(E,S) = \begin{pmatrix} M^{\ell_{\max}}(E,S) & M_a^{\ell_{\max}} \\ M_b^{\ell_{\max}} & M_c^{\ell_{\max}} \end{pmatrix} \tag{32}$$

and multiply it by the matrices P and P^T,

$$\begin{pmatrix} P^T & 0 \\ 0 & I \end{pmatrix} \begin{pmatrix} M^{\ell_{\max}}(E,S) & M_a^{\ell_{\max}} \\ M_b^{\ell_{\max}} & M_c^{\ell_{\max}} \end{pmatrix} \begin{pmatrix} P & 0 \\ 0 & I \end{pmatrix}$$

$$= \begin{pmatrix} \alpha^{\ell_{\max}}(E) & P^T M_a^{\ell_{\max}} \\ M_b^{\ell_{\max}} P & M_c^{\ell_{\max}} \end{pmatrix} , \tag{33}$$

where I represents a unit matrix, and $\alpha^{\ell_{\max}}(E)$ is a diagonal matrix containing $\alpha_i^{\ell_{\max}}(E)\delta_{i,j}$.

We show in Appendix A that for sufficiently large ℓ, the inverse t matrix, m_ℓ, can be written as a product of two factors, one which is strongly dependent on ℓ and on E, but is independent of the potential (except for its radius) and a second factor which depends on the details of the potential but is only weakly dependent on ℓ and E,

$$m_\ell(E) \approx \frac{[(2\ell+1)!!]^2}{(\kappa r^0)^{2\ell+1} P(\ell,E)} . \tag{34}$$

For a square-well potential with depth V and radius r^0, $P(\ell,E)$ is

$$P(\ell,E) = \frac{V(r^0)^2}{2\ell+3} + O(\ell^{-2}) \tag{35}$$

and for the truncated Coulomb potential it is given by

$$P(\ell,E) = \frac{Zr^0\sqrt{2Z/r^0 - E}}{(2\ell+1)(2\ell+3)} + (\text{higher-order terms in } 1/\ell) . \tag{36}$$

Similarly, it is shown in Appendix B that when ℓ and ℓ' are both large, the structure factors, $g_{\ell,\ell'}(E,S)$ may be written as

$$g_{\ell,\ell'}^m(E,S) \approx (-1)^{\ell+m} 2 \left(\frac{\ell+\ell'}{\pi}\right)^{1/2} \frac{(2\ell+2\ell'-1)!!}{(\kappa S)^{\ell+\ell'+1}} . \tag{37}$$

Clearly, for large ℓ, we have

$$|g_{\ell,\ell'}^m(E,S)|^2 \ll |m_\ell(E) m_{\ell'}(E)| . \tag{38}$$

In other words, the matrix $M(E,S)$ is nearly diagonal for high angular momentum states. This allows us to use perturbation theory to evaluate $\alpha_0^\infty(E)$. We note that $\alpha_0^{\ell_{\max}}(E_{\ell_{\max}}) = 0$, and use Eq. (33), to obtain

$$\alpha_0^\infty(E_{\ell_{\max}}) = -\sum_{\ell>\ell_{\max}} \frac{(P^T M_a^{\ell_{\max}})_{0,\ell}(M_b^{\ell_{\max}} P)_{\ell,0}}{M_{\ell,\ell}(E,S)}$$

$$= -\sum_{\ell>\ell_{\max}} \frac{\left(\sum_{\ell'=0}^{\ell_{\max}} (-1)^{\ell'} g_{\ell,\ell'}^m(E,S) b_{\ell'}^A(\ell_{\max})\right)^2}{M_{\ell,\ell}(E,S)}$$

$$= -\sum_{\ell>\ell_{\max}} m_\ell^A [b_\ell^A(\ell_{\max})]^2 . \tag{39}$$

In order to estimate α_0, we need an estimate for $b_\ell^A(\ell_{\max})$. Equation (23) which may be written

$$\frac{b_\ell^A(2\ell+1)!!}{(\kappa r^0)^\ell} = \frac{(\kappa r^0)^{\ell+1}}{(2\ell+1)!!} P(\ell) \sum_{\ell'=0}^{\ell_{\max}} g_{\ell,\ell'}^m(E,S)(-1)^{\ell'} b_{\ell'}^A \tag{40}$$

suggests an ansatz of the form

$$b_\ell^A(\ell_{\max}) \approx \frac{x^{\ell-\ell_0} Y_{\ell,0}(-\hat{\mathbf{z}})}{(2\ell-2\ell_0+1)!!}$$

$$\approx 2^{\ell_0} \frac{d^{\ell_0}}{d\,x^{\ell_0}} j_\ell(x) Y_{\ell,0}(-\hat{\mathbf{z}}) , \tag{41}$$

where x is to be determined, ℓ_0 is the angular momentum of the corresponding single-scatterer state, and $b_{\ell_0}^A(\ell_{\max}) = Y_{\ell_0,0}(-\hat{\mathbf{z}})$. For the moment we consider only σ, $(m=0)$, states.

Substituting Eq. (41) into (40), we obtain

$$\frac{x^{\ell-\ell_0}}{(2\ell-2\ell_0+1)!!} \approx \frac{(\kappa r^0)^{2\ell+1} P(\ell,E)}{[(2\ell+1)!!]^2} 2^{\ell_0} \frac{d^{\ell_0}}{d\,x^{\ell_0}} h_\ell(\kappa S - x)$$

$$\approx \frac{(\kappa r^0)^{2\ell+1} P(\ell,E)}{[(2\ell+1)!!]^2} \frac{(2\ell+2\ell_0-1)!!}{(\kappa S - x)^{\ell+\ell_0+1}} , \tag{42}$$

where we have used the expansion property of $h_\ell Y_L$. We have also omitted terms containing $b_{\ell_i}^A(\ell_{\max})$ for $\ell_i < \ell_0$, since these terms scale as $(r^0)^{2\ell+1}/S^{\ell+1}$, a much smaller ratio than that on the right-hand side (rhs) of Eq. (42). If we denote $x/(\kappa r^0)$ by ζ, we can write this approximate equality as

$$\zeta^{\ell-\ell_0}(S/r^0 - \zeta)^{\ell+\ell_0+1} \approx \frac{P(\ell,E)}{2\ell+1} . \tag{43}$$

Now the rhs of this expression vanishes as $\ell \to \infty$ as a low power of $1/\ell$. The lhs, however, either grows or vanishes exponentially depending on whether the quantity $\zeta(S/r^0 - \zeta)$ is smaller or larger than unity. This inconsistency can be resolved only if ζ has a very weak ℓ dependence. Therefore, the solution for x or ζ is given by

$$\zeta \approx \frac{S}{2r^0} - \sqrt{(S/2r^0)^2 - \ell^{-2/\ell}} . \tag{44}$$

In solving Eq. (43) for ζ we have assumed that $P(\ell)$ is

proportional to $1/\ell$ in the limit of large ℓ, and that a constant c raised to the power $1/\ell$ can be approximated by unity. We have also assumed that the expansion property of $h_\ell Y_L$ used in Eq. (42) remains valid despite the very weak ℓ dependence of x. For the case of the truncated Coulomb potential and (we presume) other potentials that have no discontinuity at the muffin-tin radius, the exponent of ℓ in Eq. (44) should be $-3/\ell$ rather than $-2/\ell$.

If $S/2r^0$ is greater than unity, ansatz (41) with $x = \kappa r^0 \zeta$ given by Eq. (44) provides an accurate representation of the leading terms describing the ℓ dependence of b_ℓ^A. If $S/2r^0$ is greater than unity and ℓ is very large, the term $\ell^{-2/\ell}$ under the radical may be approximated by unity, making ζ independent of ℓ. The ℓ dependence of ζ is also described well, for sufficiently large values of ℓ. These results are illustrated in Fig. 6 which shows $\zeta(\ell)$ as calculated, i.e., $b_\ell^A(2\ell+1)!!/(\kappa r^0)^\ell$, and as predicted, for the $1\sigma_g$ state of the spherical square wells.

If $S/2r^0$ is equal to unity, the ℓ dependence of ζ becomes significant. However, in this case, even though ζ always varies slowly with ℓ, Eq. (43) would still hold approximately if ζ were approximately equal to unity because the summation of Eq. (40) into a Hankel function has its major contributions from the terms near $\ell' \approx \ell$ when $\zeta = 1$. Since, however, ζ is smaller than unity, Eq. (44) overestimates its size. This can be seen in the uppermost curves of Fig. 6 where the calculated and predicted values of ζ are shown for the $1\sigma_g$ state calculated using touching (S=2) spherical square-well potentials. For $\ell_{\max}$ between 80 and 180, Eq. (44) overestimates ζ by an essentially constant factor of approximately 1.1.

Combining Eqs. (44), (41), and (39), we have

$$\alpha_0^\infty(E_{\ell_{\max}}) \sim \frac{-1}{4\pi\kappa r^0} \sum_{\ell>\ell_{\max}} \frac{\zeta^{2\ell}(2\ell+1)}{P(\ell)} \tag{45}$$

which can be used to estimate the error in the energy.

If $S > 2r^0$, ζ becomes independent of ℓ for sufficiently large $\ell_{\max}$. In this case Eq. (45) can be summed with the result that the error in the energy is predicted to decrease exponentially with $\ell_{\max}$,

$$E_{\ell_{\max}} - E_\infty \propto \zeta^{2\ell_{\max}} \text{ as } \ell_{\max} \to \infty . \tag{46}$$

In the special case of $S = 2r^0$, Eq. (44) reduces to

$$\zeta = 1 - \sqrt{1-\ell^{-2/\ell}} \approx e^{-\sqrt{2\ln\ell/\ell}} \tag{47}$$

although, as mentioned above this result overestimates ζ and understates the convergence rate. Using this result in Eq. (45) yields

$$\alpha_0^\infty(E_{\ell_{\max}}) \sim \frac{-1}{4\pi\kappa r^0} \sum_{\ell>\ell_{\max}} \frac{e^{-2\sqrt{2\ell\ln\ell}}(2\ell+1)}{P(\ell)} \tag{48}$$

which indicates a slower than exponential convergence. The series *does* converge however since it is easily bounded by the series

$$\sum_{\ell>\ell_{\max}} \ell^2 e^{-2\sqrt{2\ell}} \sim \sqrt{1/2}\,\ell_{\max}^{5/2} e^{-2\sqrt{2\ell_{\max}}} . \tag{49}$$

This result should not be used to estimate the convergence rate since the true convergence rate is much faster.

In the case of antisymmetric states, b_ℓ^A can change sign with increasing ℓ. This complicates the expression for b_ℓ^A. However, we found in our calculations that Eq. (44) still gives a good estimate of the magnitude of b_ℓ^A in the large ℓ limit, and therefore Eq. (45) can also be used for the antisymmetric states. The effect of $m \neq 0$ is the introduction of a factor of $(-1)^m$ on the right-hand side of Eq. (42). The effect of this factor would be to interchange the behavior of the *gerade* and *ungerade* states. Thus the $1\sigma_g$ and $1\pi_u$ states and the $1\sigma_u$ and $1\pi_g$ states behave similarly in their convergence properties.

The error in the wave function can be expressed in terms of the mismatch between Ψ_{IA} [Eq. (3)] and Ψ_{II} [Eq. (4)] at the surface of muffin tin A. Since Ψ_{IIA} [Eq. (6)] matches Ψ_{IA} identically, term by term and both value and derivative at the muffin-tin radius, we can write the error in the wave function as

$$\begin{aligned}\Delta\Psi(\ell_{\max}) &= \Psi_{IIA}(\ell_{\max}) - \Psi_{II}(\ell_{\max}) \\ &= \sum_{\ell=0}^{\ell_{\max}} b_\ell^A m_\ell^A \tilde{j}_\ell(\kappa r_A) Y_L(\hat{\mathbf{r}}_A) \\ &\quad - \sum_{\ell'=0}^{\ell_{\max}} b_{\ell'}^B \tilde{h}_{\ell'}(\kappa r_B) Y_{L'}(\hat{\mathbf{r}}_B) .\end{aligned} \tag{50}$$

After expanding the Hankel function using Eq. (12) we have

$$\begin{aligned}\Delta\Psi(\ell_{\max}) &= \sum_{\ell=0}^{\ell_{\max}} m_\ell^A b_\ell^A \tilde{j}_\ell(\kappa r_A) Y_L(\hat{\mathbf{r}}_A) \\ &\quad - \sum_{\ell=0}^{\infty} \tilde{j}_\ell(\kappa r_A) Y_L(\hat{\mathbf{r}}_A) \left(\sum_{\ell'=0}^{\ell_{\max}} g_{\ell,\ell'}^m b_{\ell'}^B \right) .\end{aligned} \tag{51}$$

The MST secular equation [Eq. (19)] (truncated at $\ell_{\max}$), can be used to eliminate the sum over ℓ' and allows the

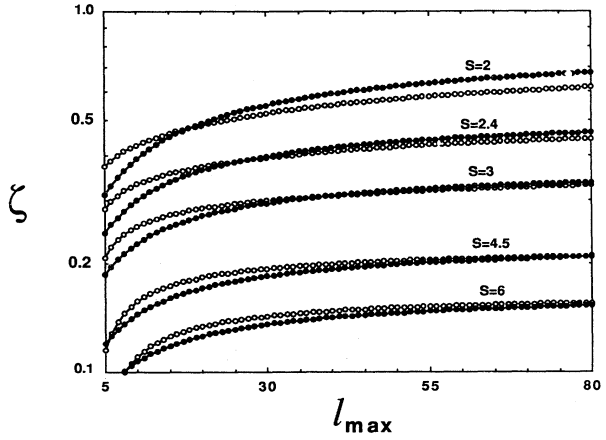

FIG. 6. Predicted (solid circles) and calculated (open circles) values of ζ, the parameter which describes the rate of convergence with $\ell_{\max}$ in MST.

cancellation of the first $(\ell_{\max}+1)$ terms in the sum over ℓ leaving

$$\Delta\Psi(\ell_{\max}) = \sum_{\ell>\ell_{\max}} \tilde{j}_\ell(\kappa r_A) Y_L(\hat{\mathbf{r}}_A) m_L^A b_\ell^A(\ell_{\max}) \ . \tag{52}$$

The average of the square of $\Delta\Psi(\ell_{\max})$ over the surface of muffin tin A is

$$\langle[\Delta\Psi(\ell_{\max})]^2\rangle = \sum_{\ell>\ell_{\max}} [\tilde{j}_\ell(\kappa r_A) m_\ell^A b_\ell^A]^2 \ , \tag{53}$$

which on substituting forms valid for large ℓ becomes

$$\langle[\Delta\Psi(\ell_{\max})]^2\rangle = (4\pi\kappa r^0)^{-2} \sum_{\ell>\ell_{\max}} (2\ell+1)\zeta^{2\ell}/P(\ell)^2 \ . \tag{54}$$

Thus the rate of convergence of the mean-square error of the wave function to zero is quite similar to the convergence of the energy to its asymptotic value, being slightly slower because $Y_L(-\hat{\mathbf{z}})^2 \sim \ell$ while $P(l)^{-2} \sim \ell^2$.

The rate of convergence of the normal derivative of the wave function can be obtained from Eq. (52),

$$\Delta\Psi'(\ell_{\max}) = \sum_{\ell>\ell_{\max}} \kappa\tilde{j}_\ell'(\kappa r_A) Y_L(\hat{\mathbf{r}}_A) m_L^A b_\ell^A(\ell_{\max}) \ , \tag{55}$$

so that in the limit of large $\ell_{\max}$ the mean-square error in the normal derivative of the wave function is

$$\langle[\Delta\Psi'(\ell_{\max})]^2\rangle = (4\pi r^0)^{-2} \sum_{\ell>\ell_{\max}} (2\ell+1)\ell^2\zeta^{2\ell}/P(\ell)^2 \ . \tag{56}$$

Thus the predicted convergence rates of the energy, the mean square error of the wave function, and the mean square error of the derivative of the wave function are all the same in the limit of $\ell_{\max} \to \infty$. These predictions are compared with the results of the numerical calculations in Fig. 7. If we define $R_p(\ell)$ to be the ratio of successive terms in the series defined by Eqs. (45), (54), and (56), we have (ignoring factors of $[\ell/(\ell+1)]^n$)

$$R_p(\ell) = [\zeta(\ell)]^{2\ell}/[\zeta(\ell+1)]^{2\ell+2} \ . \tag{57}$$

These predicted ratios are plotted as the solid curves without symbols in Fig. 7 and may be compared with the corresponding ratios calculated numerically and defined by

$$R_c^E(\ell) = \frac{E(\ell_{\max}) - E(\ell_{\max}-1)}{E(\ell_{\max}+1) - E(\ell_{\max})} \tag{58}$$

for the energy, by

$$R_c^\Psi(\ell) = \frac{\langle[\Delta\Psi(\ell_{\max})]^2\rangle - \langle[\Delta\Psi(\ell_{\max}-1)]^2\rangle}{\langle[\Delta\Psi(\ell_{\max}+1)]^2\rangle - \langle[\Delta\Psi(\ell_{\max})]^2\rangle} \tag{59}$$

for the wave function, and by

$$R_c^{\Psi'}(\ell) = \frac{\langle[\Delta\Psi'(\ell_{\max})]^2\rangle - \langle[\Delta\Psi'(\ell_{\max}-1)]^2\rangle}{\langle[\Delta\Psi'(\ell_{\max}+1)]^2\rangle - \langle[\Delta\Psi'(\ell_{\max})]^2\rangle} \tag{60}$$

for the normal derivative of the wave function. Results are shown for the $1\sigma_g$ state and the $1\pi_u$ state for the sperical square wells and for the $1\sigma_g$ state for the truncated Coulomb potentials. For the latter case $\ell^{-3/\ell}$ was used under the radical sign in calculating ζ via Eqs. (44) and (47) for the reasons described above.

The agreement between the analytical predictions of the convergence rates and those calculated is quite good. Generally, the observed convergence rates are slightly higher than those predicted. The predicted convergence rate is particularly conservative for the case of touching spheres, a result which may be traced back to the fact that Eq. (44) overestimates ζ for this case. Note that larger numbers in Fig. 7 mean faster convergence. A ratio of 10, for example, means that each succeeding term is decreasing by that factor. Constant ratios indicate exponential convergence which is observed asymptotically in all cases except for touching spheres.

The observation that exponential convergence (i.e., error $\sim e^{-a\ell_{\max}}$ where a is a constant) is not obtained for touching spheres raises the question of what happens to the convergence of the MST equations when the spheres overlap. We have not done a careful study of this case since MST does not rigorously apply to this situation. We expect, however, from Eq. (44) that the MST bound-state energies will not converge with $\ell_{\max}$ for overlapping spheres. We have performed a limited number of calculations which indicate that this is in fact the case. The asymptotic nature of the procedure only becomes apparent at fairly high values of $\ell_{\max}$ if the overlap is small.

V. CONCLUSIONS AND DISCUSSION

We have shown by direct calculation that MST can be used to obtain an extremely accurate solution to the Schrödinger equation for the case of muffin-tin potentials. We have also derived analytic formulas for the rate of convergence of these solutions as a function of $\ell_{\max}$, the total number of angular momentum states used in the calculation. Both the numerical and analytical results indicate that the errors in the wave function and its derivative decrease exponentially with $\ell_{\max}$ in the limit in which $\ell_{\max}$ is large provided there is a finite separation between the muffin-tin potentials. According to our analytic results the error in the wave function or its derivative evaluated at the muffin-tin radius decreases by the factor ζ given by Eq. (43) when $\ell_{\max}$ increases by unity. The error in the energy decreases by the square of this factor when $\ell_{\max}$ increases by unity.

In the limit of large $\ell_{\max}$, the convergence factor ζ is a function of S/r^0, the ratio of the separation between the potentials to the muffin-tin radius, and thus depends only on geometry, not on the details of the potential. The details of the potential do, however, affect the rate at which the actual convergence rate approaches the asymptotic rate,

$$\zeta_\infty = \frac{S}{2r^0} - \sqrt{(S/2r^0)^2 - 1} \ . \tag{61}$$

The *approach* to the asymptotic convergence rate is also

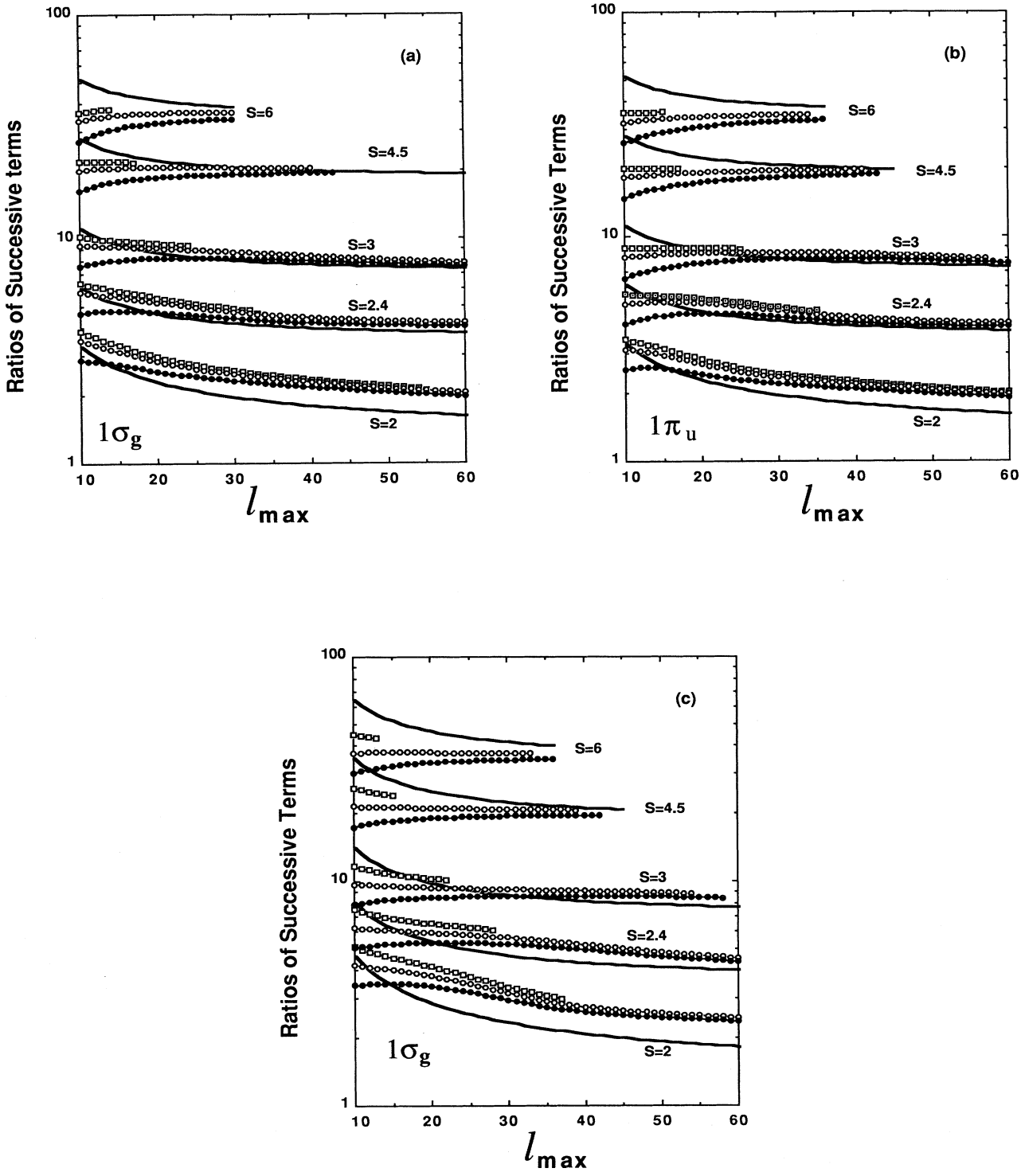

FIG. 7. Predicted (solid lines) and calculated values for the ratios $f[(\ell_{\max}) - f(\ell_{\max} - 1)]/f[(\ell_{\max} + 1) - f(\ell_{\max})]$ where f represents the energy (squares), mean square error in the wave function (open circles), or mean square error in the normal derivative of the wave function (filled circles). Panel (a) shows results for the $1\sigma_g$ state calculated for two spherical square-well potentials, panel (b) shows results for the $1\pi_u$ state for square-well potentials, and panel (c) shows results for the $1\sigma_g$ state for two truncated Coulomb potentials.

strongly dependent on the value S/r^0. As $S/2r^0$ approaches unity (the case of touching muffin tins), higher values of $\ell_{\max}$ are required to attain the asymptotic regime. For the case of $S/2r^0 = 1$, the asymptotic regime characterized by exponential convergence is never attained. MST is, however, exact and convergent even in this case.

Our results do not appear to be consistent with recent claims by Badralexe and Freeman that MST does not yield correct solutions to the Schrödinger equation for muffin-tin potentials. It is our opinion, however, that these claims are unfounded. Badralexe and Freeman reached their conclusions concerning the errancy of MST through the following line of reasoning: They treated two muffin-tin potentials by representing the wave function as a multipole expansion about the center of potential A and also as a multipole expansion about the center of potential B. By requiring that these expansions be equivalent in the interstitial region they were able to derive the MST equations. When they attempted to derive the MST equations by matching expansions inside one of the potentials, they were unsuccessful and from their lack of success concluded that MST is incorrect. They did not show any inconsistency between the expansions, merely an inability on their part to demonstrate the expansions to be equivalent. In our opinion, nothing of consequence concerning MST can be concluded from their lack of success in this endeavor.

In the most recent Badralexe-Freeman paper[10] special emphasis is placed on errors which they believe to exist in the *derivative* of the wave function. According to our calculations and analysis there is no problem peculiar to the derivative of the wave function. Its convergence properties are qualitatively very similar to those of the wave function.

ACKNOWLEDGMENTS

This work was supported by the U.S. Department of Energy Division of Materials Sciences through Contract No. DE-AC05-84OR21400 with Martin Marietta Energy Systems and through Contract No. W-7405-ENG-48 with Lawrence Livermore National Laboratory. W.H.B. gratefully acknowledges the hospitality of Lawrence Livermore National Laboratory and helpful conversations with A. Gonis of that institution. Some of the numerical calculations described here were performed using facilities of the National Energy Research Computing Center.

APPENDIX A

The inverse t matrix defined in Eq. (8) may be simplified if ℓ is sufficiently large. In order to demonstrate this simplification it is convenient to write Eq. (8)as

$$m_\ell = -\left(\frac{\gamma_\ell^{\tilde{h}} - \gamma_\ell^R}{\gamma_\ell^{\tilde{j}} - \gamma_\ell^R}\right)\frac{\tilde{h}_\ell}{\tilde{j}_\ell} , \tag{A1}$$

where the various logarithmic derivatives are defined by

$$\gamma_\ell^{\tilde{h}} = z^0\tilde{h}_\ell'(z^0)/\tilde{h}_\ell(z^0) = \ell - z^0\tilde{h}_{\ell+1}/\tilde{h}_\ell , \tag{A2}$$

$$\gamma_\ell^{\tilde{j}} = z^0\tilde{j}_\ell'(z^0)/\tilde{j}_\ell(z^0) = \ell + z^0\tilde{j}_{\ell+1}/\tilde{j}_\ell , \tag{A3}$$

and

$$\gamma_\ell^R = r_n^0\left(\frac{dR_\ell(r,E)/dr}{R_\ell(r,E)}\right)_{r=r^0} . \tag{A4}$$

For square-well potentials the logarithmic derivative of the radial wave function, is given by

$$\gamma_\ell^R = z_s j_\ell'(z_s)/j_\ell(z_s) = \ell - z_s j_{\ell+1}(z_s)/j_\ell(z_s) , \tag{A5}$$

where $z_s = \sqrt{E+V}r^0$.

The analogous relation for the truncated Coulomb potential is obtained from the analytic continuation of the standard Coulomb wave functions to imaginary argument. The radial wave function for this potential which we represent by $f_\ell(z)$ is related to the the regular Coulomb wave function[15] by

$$f_\ell(z) = F_\ell(-iZ/\kappa_c, iz) , \tag{A6}$$

where Z is the nuclear charge in units of the charge on a proton and $\kappa_c^2 = 2Z/r^0 - E$, the energy relative to the shifted potential. Thus, using $\eta = Z/\kappa_c$ and $z_c = \kappa_c r^0$ we have

$$\begin{aligned}\gamma_\ell^R &= z_c f_\ell'(z_c)/f_\ell(z_c) \\ &= l + z_c\eta/(\ell+1) \\ &\quad + z_c\left[1 - \left(\frac{\eta}{\ell+1}\right)^2\right]^{1/2} f_{\ell+1}(z_c)/f_\ell(z_c) .\end{aligned} \tag{A7}$$

In the limit of large ℓ these logarithmic derivatives can be approximated by

$$\gamma_\ell^{\tilde{h}} \to -(\ell+1) , \quad \ell \gg \kappa r^0 ; \tag{A8}$$

$$\gamma_\ell^{\tilde{j}} \to \ell - E(r^0)^2/(2\ell+3) , \quad \ell \gg \kappa r^0 ; \tag{A9}$$

and for square-well potentials

$$\gamma_\ell^R \to \ell - (E+V)(r^0)^2/(2\ell+3) , \quad \ell \gg \sqrt{E+V}r^0 ; \tag{A10}$$

while for the truncated Coulomb potentials

$$\gamma_\ell^R \to \ell + y + (z_c - y)^{1/2}(z_c + y)^{3/2}/(2\ell+1) , \quad \ell \gg \kappa_c r^0 ; \tag{A11}$$

where $y = z_c\eta/(\ell+1)$.

The approximate expression for m_ℓ for square-well potentials given in the text [Eqs. (34) and (35)] follows from substituting Eqs. (A8)–(A10) in Eq. (A1). The analogous expression for the truncated Coulomb potential is obtained by using Eq. (A11) for γ^R and is given by

$$\frac{[(2\ell+1)!!]^2}{\left(\frac{E(r^0)^2}{2\ell+3} + y + \frac{(z_c-y)^{1/2}(z_c+y)^{3/2}}{2\ell+1}\right)(\kappa r^0)^{2\ell+1}} \tag{A12}$$

which in the limit of large ℓ can be approximated by Eqs. (34) and (36).

APPENDIX B

The structure constants $g^m_{\ell,\ell'}$ satisfy the following expansion property:

$$g^m_{\ell,\ell'}(R-r)=\sum_{\ell''} f^m_{\ell,\ell''}(r)g^m_{\ell'',\ell'}(R)\ , \tag{B1}$$

where both vectors $\mathbf{R}$ and $\mathbf{r}$ are along the z axis and the matrix $f^m_{\ell,\ell'}(r)$ is defined by

$$f^m_{\ell,\ell'}(r)=(-1)^{\ell-\ell'}\sqrt{(2\ell+1)(2\ell'+1)} \times\sum_{\ell''=|\ell-\ell'|}^{\ell+\ell'}(2\ell''+1)d^m(\ell,\ell',\ell'')\tilde{j}_{\ell''}(\kappa r)\ . \tag{B2}$$

Now we use

$$\tilde{j}_\ell(\kappa r)\to\frac{(\kappa r)^\ell}{(2\ell+1)!!}\quad\text{as}\quad r\to 0 \tag{B3}$$

and

$$d^m(\ell,\ell-1,1)=\frac{\sqrt{(\ell-m)(\ell+m)}}{(2\ell-1)(2\ell+1)} \tag{B4}$$

to obtain

$$\left.\frac{df^m_{\ell,\ell'}(r)}{dr}\right|_{r=0}=-\kappa\left[\left(\frac{(\ell-m)(\ell+m)}{(2\ell-1)(2\ell+1)}\right)^{1/2}\delta_{\ell,\ell'+1} +\left(\frac{(\ell'-m)(\ell'+m)}{(2\ell'-1)(2\ell'+1)}\right)^{1/2}\delta_{\ell+1,\ell'}\right]. \tag{B5}$$

We take the derivative of Eq. (B1),

$$\frac{dg^m_{\ell,\ell'}(R)}{dR}=-\left.\frac{dg^m_{\ell,\ell'}(R-r)}{dr}\right|_{r=0}=-\sum_{\ell''=|\ell-\ell'|}^{\ell+\ell'}\left.\frac{df^m_{\ell,\ell''}(r)}{dr}\right|_{r=0}g^m_{\ell'',\ell'}(R)$$
$$=\kappa\left[\left(\frac{(\ell-m)(\ell+m)}{(2\ell-1)(2\ell+1)}\right)^{1/2}g^m_{\ell-1,\ell'}(R)+\left(\frac{(\ell-m+1)(\ell+m+1)}{(2\ell+1)(2\ell+3)}\right)^{1/2}g^m_{\ell+1,\ell'}(R)\right] \tag{B6}$$

to obtain a recursion relation for $g^m_{\ell,\ell'}$,

$$g^m_{\ell+1,\ell'}(R)=\left(\frac{(2\ell+1)(2\ell+3)}{(\ell-m+1)(\ell+m+1)}\right)^{1/2}\frac{dg^m_{\ell,\ell'}(R)}{d(\kappa R)}-\left(\frac{(2\ell+3)(\ell-m)(\ell+m)}{(2\ell-1)(\ell-m+1)(\ell+m+1)}\right)^{1/2}g^m_{\ell-1,\ell'}(R)\ . \tag{B7}$$

We have for $\ell=m$,

$$g^m_{m,\ell'}(R)=(-1)^m\sqrt{(2m+1)(2\ell'+1)} \times\sum_{\ell''=\ell'-m}^{\ell'+m}(2\ell''+1)d^m(m,\ell',\ell'')\tilde{h}_{\ell''}(\kappa R)\ , \tag{B8}$$

from which all $g^m_{\ell,\ell'}$ can be obtained. In the large-ℓ limit, with the azimuthal quantum number m fixed, the dominant term in the above equation comes from $\ell''=\ell'+m$, for which

$$d^m(m,\ell',\ell'+m) =\frac{(-1)^m(2\ell'-1)!!}{(2\ell'+2m-1)!!} \times\left(\frac{(2\ell'+1)(2m+1)!!(\ell'+m)!}{(2\ell'+2m+1)(2m)!!(\ell'-m)!}\right)^{1/2} \tag{B9}$$

and therefore we obtain the approximate expression

$$g^m_{m,\ell'}(R)\approx\left(\frac{(2\ell'+1)!!(2\ell'-1)!!(2m+1)!!}{(\ell'+m)!(\ell'-m)!(2m)!!}\right)^{1/2} \times\frac{1}{(\kappa R)^{\ell'+m+1}}\ . \tag{B10}$$

In the limit $\ell\gg m$, the recursion relation for $g^m_{\ell,\ell'}$ yields

$$g^m_{\ell,\ell'}(R)\approx\left(\frac{(2\ell-1)(2\ell+1)}{(\ell-m)(\ell+m)}\right)^{1/2}\frac{dg^m_{\ell-1,\ell'}(R)}{d(\kappa R)} \approx\frac{(2\ell-1)!!}{(2m-1)!!}\left(\frac{(2\ell+1)(2m)!}{(2m+1)(\ell-m)!(\ell+m)!}\right)^{1/2} \times\frac{d^{\ell-m}g^m_{m,\ell'}(R)}{d(\kappa R)^{\ell-m}}\ . \tag{B11}$$

Substituting in Eq. (B10) and using the Stirling formula for the factorials, one immediately obtains Eq. (37) for $g^m_{\ell,\ell'}$.

[1] Lord Rayleigh, Philos. Mag. **34**, 481 (1892).
[2] J. Korringa, Physica **13**, 392 (1947).
[3] W. Kohn and N. Rostoker, Phys. Rev. **94**, 1111 (1954).
[4] K. H. Johnson, J. Chem. Phys. **45**, 3085 (1966).
[5] J. C. Slater, *Solid State and Molecular Theory: A Scientific Biography* (Wiley, New York, 1975).
[6] W. H. Butler and R. K. Nesbet, Phys. Rev. B **42**, 1518 (1990).
[7] A. Gonis, X.-G. Zhang, and D. M. Nicholson, Phys. Rev. B **40**, 947 (1989).
[8] E. Badralexe and A. J. Freeman, Phys. Rev. B **37**, 10 469 (1988).
[9] A. Gonis, R. Zeller, P. H. Dederichs, J. S. Faulkner, B. L. Gyorffy, D. M. Nicholson, G. M. Stocks, L. T. Wille, and X.-G. Zhang, Phys. Rev. B **41**, 10 224 (1990).
[10] E. Badralexe and A. J. Freeman, Phys. Rev. B **41**, 10 226 (1990).
[11] W. H. Butler, Phys. Rev. B **41**, 2684 (1990).
[12] The function m_ℓ defined by Eqs. (7) and (8) is related to the t matrix of scattering theory by $m_\ell = (-)^\ell t_\ell^{-1}/\sqrt{-E}$.
[13] This problem corresponds to an *elliptic* equation with *Dirichlet* boundary conditions for a *closed* surface. It is well known that such problems have a unique well-defined solution. P. M. Morse and H. Feshbach, *Methods of Theoretical Physics* (McGraw-Hill, New York, 1953), p. 706.
[14] J. C. Slater, *Quantum Theory of Molecules and Solids* (McGraw Hill, New York, 1963), Vol. 1, pp. 5–7.
[15] *Handbook of Mathematical Functions*, edited by M. Abramowitz and I. A. Stegun (U.S. GPO, Washington, D.C., 1965, also reprinted by Dover, New York), p. 538.